Article citation info:
Chen X, Cheng X, Wu N, Liu X. Unmanned aerial vehicle transmission defect detection technology based on edge computing. Diagnostyka. 2024;25(4):2024408. https://doi.org/10.29354/diag/194598.



**DIAGNOSTYKA**, 2024, Vol. 25, No. 4

**e-ISSN** 2449-5220
**DOI:** 10.29354/diag/194598

# UNMANNED AERIAL VEHICLE TRANSMISSION DEFECT DETECTION TECHNOLOGY BASED ON EDGE COMPUTING

**Xi CHEN *, Xumeng CHENG, Nengcheng WU, Xuanyou LIU**

Fangchenggang Power Supply Bureau of Guangxi Power Grid Co., Ltd, Fangchenggang, 538001, China
* Corresponding author, e-mail: leng909210257@126.com

Abstract

Defect identification of transmission lines has become a crucial step in ensuring the proper functioning of the current transmission system due to the ongoing growth of the power grid size. The study primarily concerns itself with the current shortcomings of unmanned aerial vehicle transmission defect detection, particularly in terms of image quality and other related issues. In response, an unmanned aerial vehicle transmission defect detection system based on edge computing has been proposed. This system employs edge computing networks and lightweight improvements, and finally, through the analysis of experimental data, the performance and detection effectiveness of the system are validated. The outcomes revealed that the accuracy of the model used for the study in detecting insulators is 0.05 higher than other models. The system was more effective in detecting normal insulators and abnormal insulators. The error of the system in detecting transmission line images was 0.18 lower than other algorithms, and the average percentage error was 0.20 lower compared to other model error values. This reveals that the system used in the study was able to improve the detection of transmission lines, and also improved the quality of the detected images. This is an excellent manual for enhancing UAV transmission line defect detection precision in the future.

Keywords: edge computing; transmission lines; unmanned aerial vehicle; defect detection; insulators

## 1. INTRODUCTION

The safe and stable functioning of transmission lines (TLs), a significant conduit for power transmission in the contemporary electric power system, is essential to the regular operation of social production and daily living [1]. However, in the natural environment, TLs are often affected by the natural environment and human factors, resulting in a variety of defects often occurring in TLs, which may lead to serious safety accidents if they are not detected and treated in time [2]. To guarantee the current functioning of the power system, it is crucial to understand how to precisely inspect TL [3]. Most of the traditional TL inspections rely on manual inspection, which is not only inefficient but also has a large security risk. Unmanned aerial vehicle (UAV) technology has advanced over time, and because of its benefits-such as improved mobility and a broad inspection range-UAVs are now a new technique for TL inspection [4]. UAV can also carry high-resolution cameras and other sensors to automate the inspection of TLs, which substantially improves the inspection efficiency and safety, while a large amount of image data processing and real-time defect detection (DD) pose a great challenge to the UAV's data processing capability. Edge computing (EC), as a new computing paradigm, can effectively reduce the computational pressure of the central cloud, reduce the data transmission delay, and realize rapid response by performing data processing at the near-end of the network edge.

DD of TL can not only guarantee the stable operation of the transmission system, but also prevent the occurrence of safety accidents. An ultra-small bolt DD model based on a deep convolutional neural network was proposed by Luo et al. to address the challenge of bolt flaws in TL detection that are hard to identify. With the help of the local bolt detection module and the ultra-small object perception module, the model was able to intelligently recognize bolt flaws. The study's findings showed that the suggested approach has significant application value and can successfully enhance bolt DD performance [5]. Dong et al. suggested a detection technique that enhances the TL image DD performance by combining CNN and Transformer. The outcomes showed that, in terms of average TL image DD correctness, the suggested method performs better than other widely used approaches [6]. To address the challenges of

Received 2024-05-28; Accepted 2024-10-14; Available online 2024-10-27

insulator DD in smart grids, Liu et al. researched and systematically sorted out the research progress of insulator defects based on deep learning, and proposed insulator processing stage methods using image preprocessing algorithms for data augmentation and underlying visual information extraction, as well as a DD stage model using different task objectives for fault localization and classification. The results of the study showed that these methods achieved significant results in improving the DD performance of insulators [7]. To accomplish the tiny surface DD task in Industry 4.0 and get around the problem of dynamic changes on the development of the relationship between the twin simulation and the real scene, Wu et al. presented a digital twin solution based on a networked manufacturing system. The novel approach efficiently collected, processed, analyzed, and stored factory data by combining edge cloud architecture and deep learning techniques. The outcomes showed that, in small-scale fault detection tasks, the suggested approach achieves good accuracy and recall [8]. The DSMH-YOLOv4 algorithm, which is based on YOLOv4, was proposed by Han et al. to increase the speed and accuracy of UAVs used to identify flaws in TL insulators. The study's findings demonstrated that the algorithm's parameters were lowered and that insulators' and faults' average accuracy increased [9]. In Kiruthiga and Prakash's study, it was found that transmission lines often experience varying degrees of potential faults and defects during operation, thus requiring detection of transmission lines at different times. Therefore, an artificial intelligence transmission line detection technology was used in the study. The new technology can use different intelligent technologies to detect transmission lines, and greatly improve the accuracy and recall of fault detection, reducing the need for manual detection [10]. Ahmed and Mohanta found that the use and manufacturing of drones are currently important issues in the high-altitude detection of transmission line faults. Therefore, a deep learning evaluation method has been proposed to be introduced into drones, which can identify relevant faults of power transmission line insulators during drone fault detection. The research results indicate that the new method can improve the effectiveness of unmanned aerial vehicles in detecting faults in transmission lines, enhance detection accuracy, and make a good contribution to the detection and evaluation of transmission line faults [11]. Benelmostafa et al. found in their study that using machine vision technology is a good detection technique for power transmission lines. Therefore, in order to improve the practical effect and accuracy of transmission line detection, a research proposes an unmanned aerial vehicle transmission line detection technology based on the Yolov8 algorithm. The new technology can fuse the components of the Yolov8 algorithm into different feature maps to enhance detection performance. The research results indicate that the new method significantly improves detection accuracy while maintaining efficiency, which has a good guiding role for the detection of unmanned aerial vehicle transmission lines [12].

It can be observed that there have been many studies conducted on TL detection research, but most of the studies have poor image processing. Based on this, the study proposes a new technique for UAV transmission detection based on EC. The study analyzes the TL images by using the Efficientdet network in EC to improve the image detection, and also improves the Efficientdet model by using the lightweight network to improve the system's ability to store and process the image data. The research is mainly divided into four parts. The first part mainly introduces the research background and current research direction; The second part mainly involves building a research system through algorithms and applying it in practice; The third part mainly verifies the feasibility of the current research model through experiments; The fourth part is a summary of the current article.

## 2. METHODS AND MATERIALS

### 2.1. Transmission defect detection algorithm based on edge computing

DD of TL mainly analyzes the current line by the image of TL, and the image is usually taken by UAV, but the resolution of the image is too large as well as the target of the current detection image is too small. Therefore, in the process of taking TL images, problems such as unclear images or inaccurate detection often occur. Therefore the study uses small target detection network model for detection analysis. Therefore the study selects Efficientnet for target detection analysis, but due to the lack of target detection accuracy in the first and second stage of the algorithm, for this reason a new BiFPN algorithm network is introduced to build a new Efficientdet model [13]. Efficientdet model has various loss definition methods in defining target loss as shown in Equation (1).

$$y_i = sigmoid(x_i) = \frac{1}{1+e^{-x_i}} \quad (1)$$

In Equation (1), $i$ is the sample, $y_i$ denotes the value of sample $i$ after activation function, and $sigmoid$ denotes the activation function. $x_i$ denotes the output value of sample $i$ in the activation function. Equation (2) displays the resulting classification loss function [14].

$$L_{class} = -\sum_{i=1}^{N} y_i^* \, log(v_i) + (1 - y_i^*) \, log(1 - y_i) \quad (2)$$

In Equation (2), $L_{class}$ denotes the value of the classification loss function $N$ denotes the total samples, and $y_i^*$ denotes the predicted value in sample B.

$$L_{local} = (h - h^*)^2 + (x - x^*)^2 + (w - w^*)^2 + (y - y^*)^2 \quad (3)$$

In Equation (3), $x^*$ denotes the horizontal coordinates of the predicted center point (PCP) in the sample and $y^*$ denotes the vertical coordinates of the PCP in the sample. $w^*$ denotes the width of the PCP in the sample and $h^*$ denotes the height of the PCP. In the algorithm detection process each wire image is regarded as a sample, the different image content is categorized into a label, and then the size and proportion of the image is divided according to the actual situation, to determine the current image proportion such as the size of 16 * 16, 32 * 32 or 64 * 64 and so on. Then the alternative image division is mapped into the BiFPN network, which is divided into different generating frames by the division rules, and then its index value is calculated. As shown in Equation (4) its metrics calculation formula [15].

$$IoU = \frac{|A \cap B|}{|A \cup B|} \quad (4)$$

In Equation (4), $A$ denotes the image to be generated and $B$ denotes the real image to be divided. $|A \cap B|$ denotes the intersection of the two image collections. $|A \cup B|$ denotes the area size of the two image collections. $IoU$ denotes the number of intersection and ratio indicators in the image. To improve the resolution of the image, the function is set as shown in Equation (5) when the algorithm is performed.

$$Y_i = F(X_i) \quad (5)$$

In Equation (5), $F$ is the convolution of the image and $Y_i$ denotes the output. $X_i$ is the output value of the image dimension, at this point the recursive operation of the algorithm is shown in Equation (6) [16].

$$N = F_k \odot F_{k-1} \odot \cdots \odot F_1 \odot F_1(X_1) = \bigodot_{j=1,2,\cdots,k} F_j(X_1) \quad (6)$$

In Equation (6), $\odot$ denotes the recursive operation, here the convolutional layer is divided into a number of different stages, each of which has the same type, at which point the convolutional model is shown in Equation (7).

$$N = \bigodot_{i=1,\cdots,s} F_i^{L_i}(X_{(H_i,W_i,C_i)}) \quad (7)$$

In Equation (7), $(H_i, W_i, C_i)$ denotes the dimensional information size of the transmission volume of the network at stage $i$. The resolution efficiency of the model for TL images can be improved by network scaling, as shown in Equation (8) for the scaling process of the model.

$$W_{bifpn} = 64*(1.35^{\varphi}) \quad (8)$$

In Equation (8), $W_{bifpn}$ denotes the number of channels of the model and $\varphi$ denotes the change in image size of the current user. The scaling process obtained by the change in the network layers is shown in Equation (9) [17].

$$D_{bifpn} = 3 + \varphi \quad (9)$$

In Equation (9), $D_{bifpn}$ denotes the convolutional layers of the model. The network model's breadth is raised to obtain the result indicated by Equation (10).

$$D_{box} = 3 + |\varphi/3| \quad (10)$$

Since more than 3 layers of feature network images are used in the main network model of the model, the resolution of the input at this point can be achieved by performing a multiplicative division as shown in Equation (11) [18].

$$D_{input} = 512 + \varphi*128 \quad (11)$$

In Equation (11), 128 denotes the multiplier to be divided, where the number of feature layers set is 7, then the multiplier is 2 to the 7th power times. Ultimately, the model applies convolution and sampling operations to the image in order to improve graphics processing and enhance pixels and data. The image processing process and pixel enhancement method is shown in Figure 1.

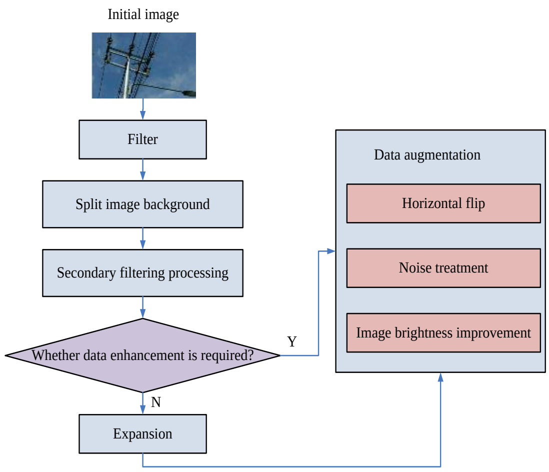


Fig. 1. Image processing and pixel enhancement methods

In Figure 1, when the TL image is input, the image is first smoothed by image filtering, followed by a morphological transformation of the image to divide the background of the image, and then the divided image is subjected to a secondary filtering process, and then a judgment is made to determine whether data enhancement detection is required. If necessary, the image is expanded and then data enhancement processing, while the data enhancement detection is not required to directly carry out data enhancement, or then the image is analyzed by background filtering. One of the data enhancement methods include level flipping, noise processing, image brightness enhancement and so on.

**2.2. Lightweight system construction based on edge computing**

As the TL model is being stored it requires the device to have a large enough memory so that the images can be stored efficiently. However, such devices will often require more complex or larger model structures, but too much storage will reduce the model recognition accuracy and model representation, so the model representation needs to be enhanced by augmenting the dataset. Lightweight network is to quantize and prune the model based on the original network. In addition, pruning is the process of filtering the fixed network model structure to remove redundant and superfluous processes. The lightweight network structure allows the network model with the same accuracy, speed and computation can be improved, as shown in Figure 2 for the basic unit structure of the lightweight network.

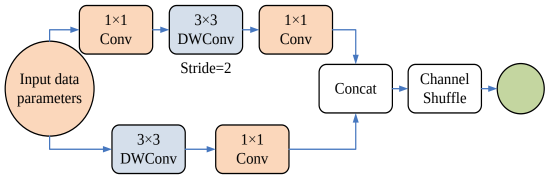


Fig. 2. Basic unit structure of lightweight network

In Figure 2, the lightweight network employs two different types of convolution methods: the first unifies the model's channels to ensure channel consistency, while the other fuses information data to enhance the model's feature information processing capability. Lastly, combining the two approaches helps speed up the model's picture processing by reducing the number of model parameters during operation. In the process of edge detection in the model needs to replace the convolutional layer of the model, such as research using the image detection algorithm Yolov2 network in the Pass Through layer of the initial network to replace the convolutional layer, and then to the new network layers in order to re-complete the convolutional operation of the model. The second is to enhance the inference effect of the model; that is, in the basic model of the various scales of the picture of the target inference, when the picture's dimensional data information is larger, the dimensionality of the vector picture is obtained as 1 * 21 * 13 * 13 by using the convolutional layer inference model [19]. However, in general, the same picture scale inference now need to minimize the amount of model computation on the picture, reduce the number of model layers, in an attempt to reduce the loss of the model due to the layers is too much, to improve the efficiency of the calculation of the picture EC is to enhance the model of the picture analysis of a tool in the analysis of the picture detection and analysis of the need to be first deployed on the edge detection equipment, as shown in Figure 3.

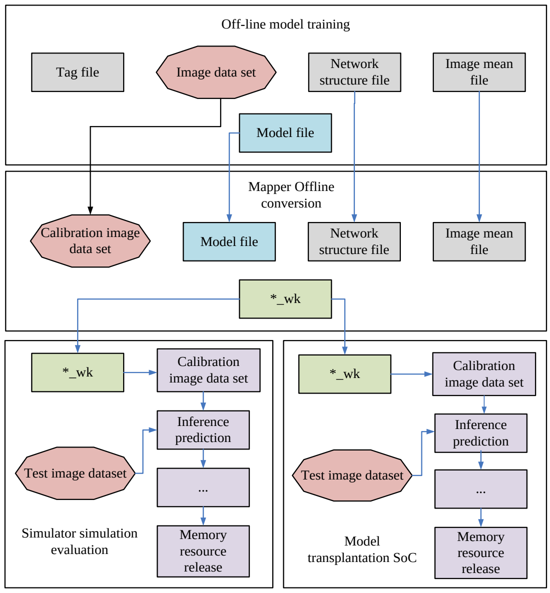


Fig. 3. Deployment process of edge detection devices

The edge detection system is deployed in four stages, as shown in Figure 3: offline processing, data transformation, data assessment, and model data transfer. The offline processing model is to analyze the image data offline and train and process the data of the image through the structure of the model. And in the offline module, the mean file, model file, and network structure file of the chip will be converted with the data conversion module, and then the image data will be converted into a calibrated image dataset. Data conversion is the process of transforming the slipper information data obtained through offline processing, so that it can be recognized and processed by the system. At the same time, a new file storage module will be added to the module to store the obtained image data for the next step of operation. Data evaluation is the process of simulating the converted data and conducting predictive analysis to release resources. And the module will also infer and predict the image data used for testing, load and release the final test image data. Model data transfer is to store the image data from the simulation so that the data can be called in a better way.

Before the analysis of the detection chip needs to be carried out on the model of the data framework processing, the quantitative processing of the picture data is divided into two parts of the file information, one is the description of the picture file data information, one is the model data file information [20-21]. Through quantization processing these two kinds of files are compressed to a smaller range, through the lightweight processing of the smear can become smaller weight value, but the overall model preservation effect will be improved, so as to achieve the effect of preservation of more data. For the EC detection system of the model needs to be deployed in several directions as shown in Figure 4.

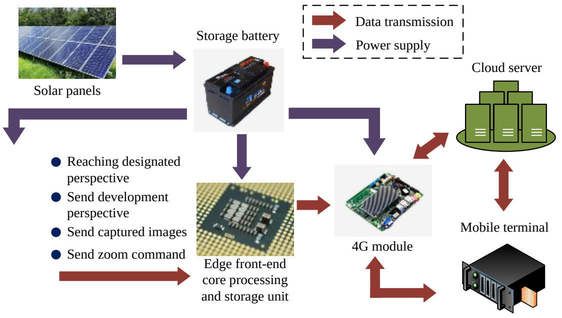


Fig. 4. Components deployed by edge computing detection system

In Figure 4, the TL image monitoring system includes a number of components such as a camera, a monitoring chip, a storage unit, a battery, a solar panel, a mobile terminal system, a storage module, and so on. The system can be able to complete the transmission of image information, specified angle rotation, signal commands issued and other operations through these components. The solar panels in the chip system provide energy for the mind, power the chip, and transmit the required data to designated components through signal instructions between various hardware components. Finally, the entire system encrypts the transmitted data to ensure data security. When the chip receives the command, it will send the high-definition picture to the main system of edge detection, and the whole system carries on the communication transmission through the chip, and transmits the picture data into the cloud server. The communication module of the system is shown in Figure 5.

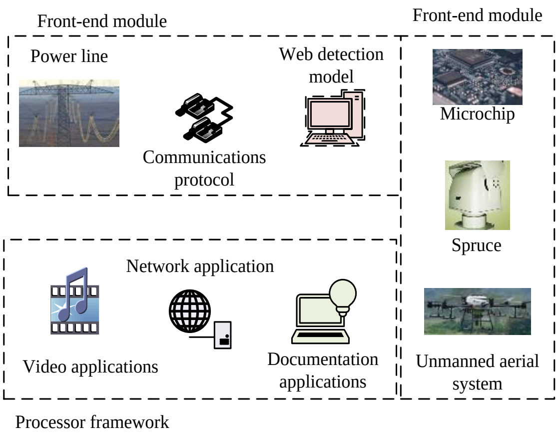


Fig. 5. System communication module

The communication system shown in Figure 5 is composed of three main modules: the data processing module, the front-end system module, the cloud control module, and the communication mechanism. The front-end system module is mainly responsible for receiving front-end data and transmitting command signals. The data processing module is mainly responsible for the unified processing and analysis of signals received through the front-end module, and transmitting them to the next communication module. The cloud control module mainly controls the instructions and signals obtained from data processing, and controls the system to transmit the next step of data signals. The communication mechanism is an important means of connecting the main system to the UAV and this mechanism mainly uses nanomsg to operate on the edge system. At the same time the system supports the connection to a single communication and is able to distribute the load in a balanced way to multiple data nodes [22]. Lastly, the system must be able to assess the state of several applications in order to ensure system reliability.

In the communication device of the system, it is necessary to connect the situation of the UAV through the cloud service and also to observe the surroundings of the TL through the camera of the UAV [23-25]. Therefore, the above mentioned EC is used in the system for the connection of the system communication. The communication protocol uses the hypertext transfer protocol, through the receipt of the request and then to the information of the system text data to broadcast, so as to respond to realize the server's response and connection. The communication connection process is shown in Figure 6.

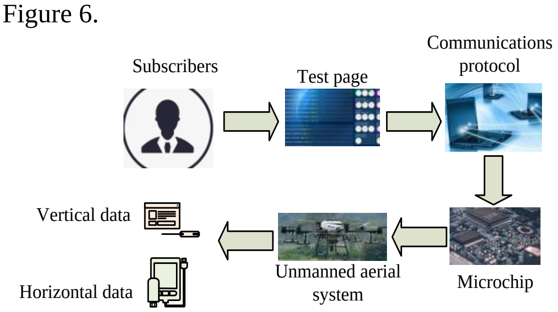


Fig. 6. Communication connection flow

In Figure 6, when the user carries out the system operation, he or she firstly needs to carry out the system operation through the system webpage, and secondly, the webpage, after receiving the data information, transmits the control information required for the operation into the control chip through the communication protocol. After receiving the signals, the control chip will return the signals from the front end to the control cloud, in which the signals from the front end include the current position information of the UAV, the horizontal status and so on. Finally, the communication signal is analyzed by EC and the current operation is executed while waiting for the next information. Thus the whole UAV TL fault detection system is built.

## 3. RESULTS OF UAV TRANSMISSION LINE DEFECT DETECTION TECHNIQUE BASED ON EDGE COMPUTING

### 3.1. Edge computing model defect detection effect analysis

To investigate the detection effect of the system and the test results of EC, the study is analyzed using the 2023 UAV TL collection data, which has 158k image data in the dataset. The data in the training, validation and test sets are distributed in the ratio of 7:1:2. A total of 36k TL are labeled. There are three types of TL type files that are labeled, which are physical labeling, key point detection of TL, and image overview of TL. The data image used for the study is the 2023 Transmission Line Insulators public dataset. The tests use detection accuracy, F1 value and recall to indicate the detection effectiveness. The DD effect of the EC system on the data images is shown in Figure 7.

In Figure 7(a), normal insulators (NIs) and insulators with defects during the detection process differ in the detection accuracy variation curve. The accuracy of NIs increases first with the increase in network score and then a gradient decreases. The accuracy of defective insulators (DI), on the other hand, stabilizes and then starts to increase and finally decreases in a straight line. The accuracy of NIs is

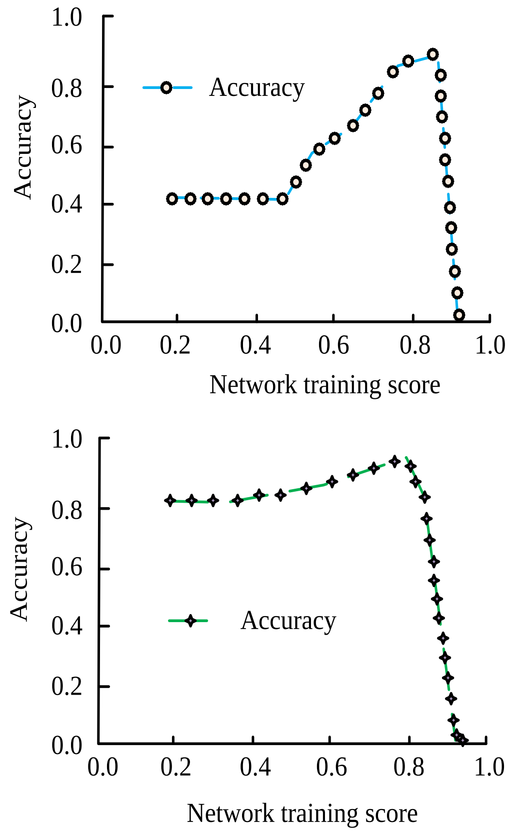


(a) Changes in insulator accuracy

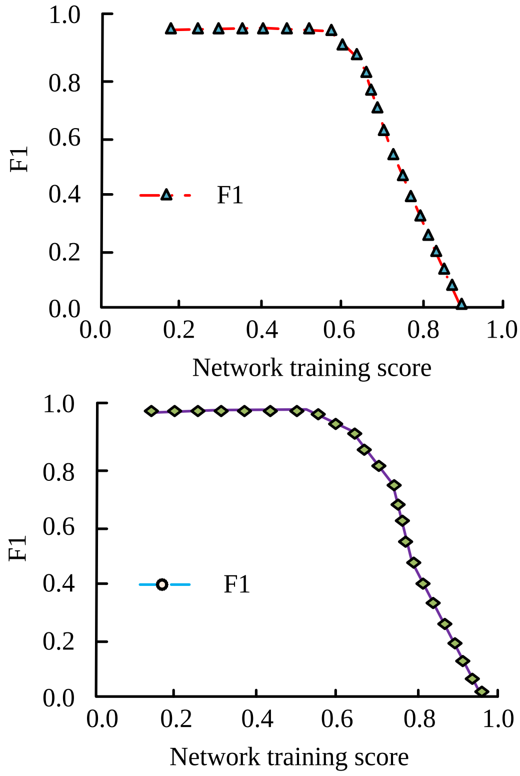


(b) F1 value change of insulator

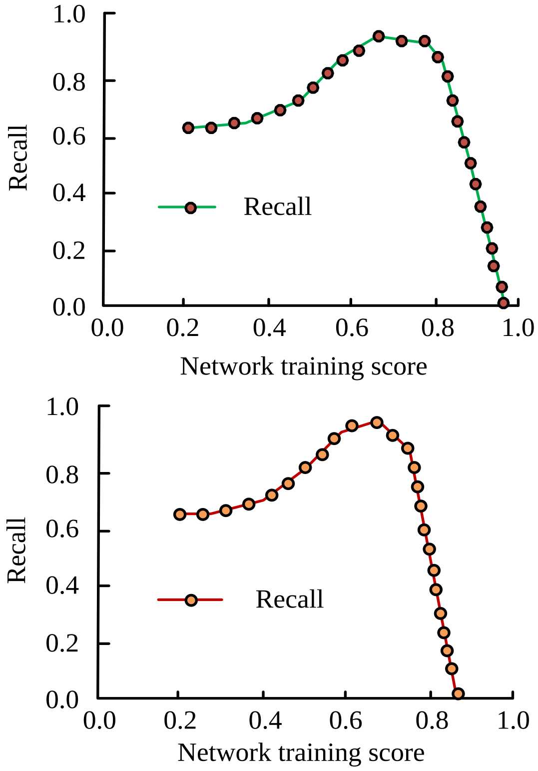


(c) Changes in insulator recall rate

Fig. 7. Comparison of detection effects between faulty insulators and normal insulators

also higher compared to DIs. The highest accuracy rate of NI is 0.94, and the highest accuracy rate of DI is 0.91, and the accuracy rate of NI is 0.03 higher than that of DI. In Figure 7(b), the change of F1 value of normal and DIs is basically the same, but the F1 value of NIs is higher with 0.97, and the F1 value of DIs is only 0.95 at the highest. The F1 value of NIs is 0.02 higher than that of DIs. insulator is 0.02 higher. In Figure 7(c), the change curves of the recall rate of NIs and DIs are basically known, but the recall rate of NIs is higher, with the highest recall rate of NIs being 0.96, and that of DIs being 0.92. The recall rate of NIs is higher than that of DIs by 0.04. It can be seen that the NIs have higher performance than the DIs in the process of testing. Figure 8 compares the data detection times for the EC model.

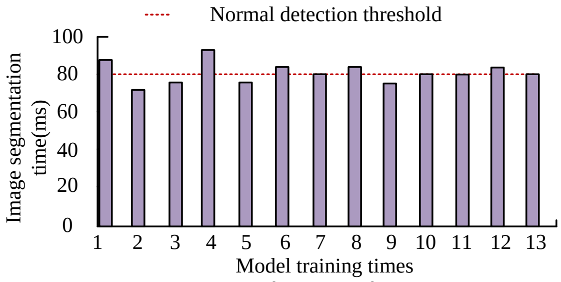

(a) Comparison of total time for model image segmentation effect

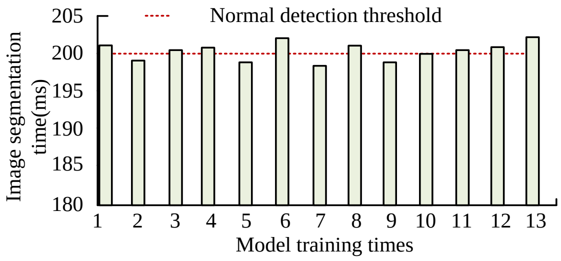

(b) Comparison of total length of image inference

Fig. 8. Comparison of edge computing model image data detection time

In Figure 8(a), the total time threshold varies between 80ms when the model is segmenting the image. However, with the increase in the training times of the model, the image segmentation time of the model starts to show up and down fluctuations, in which the shortest segmentation time is 66ms, the longest segmentation time is 92ms, and there is a difference of 26ms between the longest and the shortest time. It can be seen that the model segmentation time varies with the change in the number of training times when segmenting an image, but the overall trend of the change is relatively stable. In Figure 8(b), in the total time of the model image segmentation its time threshold is 200ms, with the increase in the training times the total time of the model began to fluctuate and change, of which the longest time is 202ms, the shortest time is 198ms, the difference between the two is 4ms. This shows that in the total time of the image segmentation changes in the model time segmentation is more effective, but also more stable. Table 1 displays the average accuracy of various techniques for insulator detection.

Table 1. Average accuracy of insulator detection by different models

| Object detection algorithm | Bolt detection and insulator detection | | |
|---|---|---|---|
| | Average accuracy | Average accuracy | Data size |
| | Image threshold 0.5 | Image threshold 0.5-0.95 | |
| Research Use Model | 0.963 | 0.862 | 13.6 M |
| Efficientdet | 0.845 | 0.603 | 108 M |
| Efficientdet+Swin Transformer | 0.934 | 0.812 | 198 M |
| yolov51+Efficientdet | 0.862 | 0.439 | 44.2 M |
| Efficientdet+GhostNet | 0.865 | 0.513 | 46.7 M |
| Efficientdet+Mobilenetv3Small | 0.832 | 0.422 | 39.1 M |
| Efficientdet+PP-LCNet-1x | 0.784 | 0.421 | 41.5 M |

In Table 1, the performance results obtained after adding different mechanisms to the Efficientdet module are not very satisfactory, where the best result obtained except the model used in the study is the addition of the attention mechanism at a picture threshold of 0.5, with an average accuracy of 0.934, which is 0.029 lower compared to the model used in the study, 0.963. This indicates that the performance results of the model after using the lightweighting better. In addition, the model with the attention mechanism is more effective than the other models when the picture threshold is between 0.5-0.95; this is 0.05 less effective than the study's model, which is 0.862.. Finally, the size of the data model obtained by the use of lightweighting is as small as 13.6, which indicates that the use of lightweighting network can significantly reduce the size of the data of the TL detection, and increase the ability to process the data.

### 3.2. Actual effect of the transmission line inspection system

The research will be processed and analyzed using the system on TPUv3 as a 64-core processor. The model is tested for data from D0 to D7, and D denotes the scaling factor of the model, and the system tested uses Windows. The graphic processor and the central processor used for the study are NVIDIA GeForce GTX1070 and Intel Core i7-7700k @ 3.7GHz respectively, and the size of the memory used is 16G and 32G. The comparison algorithms are selected for the comparison analysis of YOLOv5x, YOLOv7x and Faster R-CNN FPN algorithms. The effect of the system NI and damaged insulator detection is shown in Figure 9.

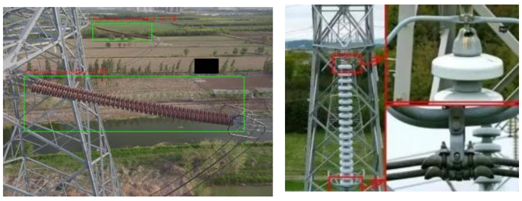

(a) Abnormal insulator detection results

(b) Normal insulator inspection diagram

Fig. 9. Comparison of inspection results of insulator systems

In Figure 9(a), when a defect is detected in the current insulator, the UAV will mark the location parts of the detected insulators that are defective and zoom in on the details so that the defective parts can be better observed. In Figure 9(b), when NIs are detected, the system used in the study will analyze the different detected parts of the insulators that are prone to defects, and at the same time process and analyze the data of their image information and upload the data so as to make a judgment on whether defects are present or not. As shown in Table 2 shows the different processing effects on the data with different scaling degrees of the system algorithm.

Table 2. Different scaling effects of system algorithms on data processing

| Model scaling factor | Average accuracy | Data parameter size | Network parameters |
|---|---|---|---|
| Efficientdet -DO | 0.339 | 2.9M | 2.4B |
| Efficientdet -D1 | 0.403 | 6.4M | 6.0B |
| Efficientdet -D2 | 0.440 | 7.9M | 11.0B |
| Efficientdet -D3 | 0.469 | 13.0M | 24.0B |
| Efficientdet -D4 | 0.501 | 20.0M | 54.0B |
| Efficientdet -D5 | 0.531 | 33.0M | 133.0B |
| Efficientdet -D6 | 0.535 | 51.0M | 224.0B |
| Efficientdet -D7 | 0.512 | 51.0M | 323.0B |

In Table 2, the average accuracy of the processed images varies in the different scaling systems of the model, where the model with scaling factor of 6 has the highest average accuracy of 0.535, which is 0.196 higher compared to the scaling system of 0, which has the lowest average accuracy. The maximum size of the processed image data is also in the scaling factors of 6 and 7. However, the size of the model network processing parameter for the model with scaling factor of 6 is only 224.0, which is 99B lower than that of the model with scaling factor of 7. It is evident that the performance of the model used in the study with scaling factor set to 6 is able to achieve better values and process more data. A comparison of the DD effect of different algorithms on insulators is shown in Figure 10.

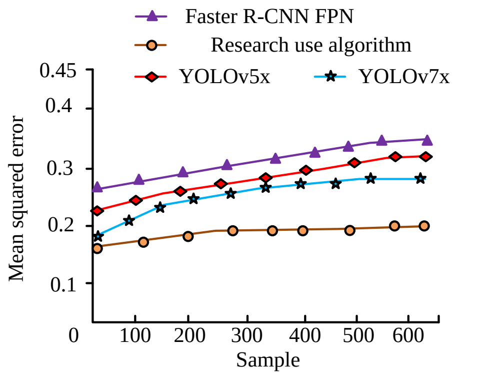


(a) Root-mean-square deviation of three algorithms

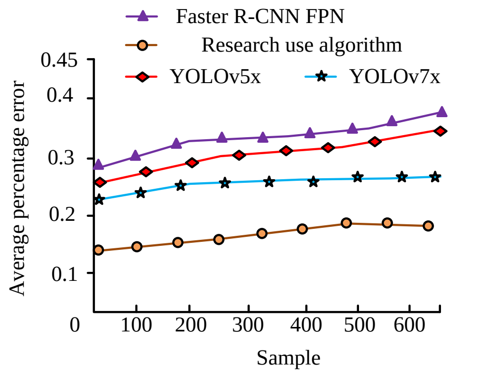


(b) Minimum error of three algorithms

Fig. 10. Comparison of detection error results for insulator systems using different algorithms

The study's root mean square error mean value varies around 0.16, compared with the highest error algorithm model Faster R-CNN FPN algorithm of 0.34, which is about 0.18 lower. In Figure 10(a), the study compares algorithms used in the root mean square error. The error value changes as the number of samples increases and essentially stays the same. Figure 10 (b), the study uses algorithms model of the average percentage error value is basically unchanged as the number of samples increases, with an average value of about 0.15, which is about 0.20 lower compared to 0.35 of the Faster R-CNN FPN algorithmic model with the highest error. It can be seen that the algorithmic model used by the study has a better detection effect on the transmission detection process.

## 4. CONCLUSION

The research mainly focuses on the current UAV transmission detection effect and the lack of image quality, and proposes an algorithmic model based on EC, and the new model uses the Efficientdet model and improves it by lightweighting. Firstly, the algorithmic model of EC is proposed, and secondly, the new UAV transmission detection system is built by lightweight improvement. The outcomes revealed that the use of the new algorithmic model has a better detection of insulators where the accuracy of detecting NIs is 0.03 higher than DIs. The F1 value of NIs was 0.02 higher than that of DIs. The model had a smaller deviation from the total length of time when segmenting the image of only 4ms, and the model had a high stability of detection. When the image threshold was 0.5, the model used in the study had an accuracy of 0.963. When the image threshold was between 0.5 and 0.95, the model with the addition of the attention mechanism was 0.05 lower than the 0.862 of the model used in the study. The system studied was able to detect and analyze NIs and abNIs in more detail. The study used a model scaling factor of 6 when the system detection is optimal, the average accuracy has 0.535, which is 0.196 higher than the model with the lowest effect scaling factor, where the size of the network parameter is 99B lower than the scaling factor of 7. Finally, the study used a model with the value of the root mean squared error is lower than the Faster R-CNN FPN algorithm by about 0.18, and the average percentage error is lower than the Faster R-CNN FPN algorithm by about 0.20. It can be concluded that the research using algorithmic model can effectively analyze the transmission detection through UAV and can achieve better detection results, while the accuracy and stability of the model maintains a good value. Although the research has achieved a lot of results, but there are still some problems, so the research will be followed by adding more different network models to improve the system. Secondly DD analysis of different transmission devices will also be carried

**Source of funding:** *The research is supported by: Guangxi Power Grid Co., Ltd. Science and Technology Project Funding, "Research on Online Defect Identification Technology for Mobile Edge End", (No. 040700KC23040002).*

**Author contributions:** *X.C. and X.M.C. processed the numerical attribute linear programming of communication big data, and the mutual information feature quantity of communication big data numerical attribute was extracted by the cloud extended distributed feature fitting method. N.C.W. combined with fuzzy C-means clustering and linear regression analysis, the statistical analysis of big data numerical attribute feature information was carried out, and the associated attribute sample set of communication big data numerical attribute cloud grid distribution was constructed. X.Y.L. did the experiments, recorded data, and created manuscripts. All authors read and approved the final manuscript.*

**Declaration of competing interest:** *The author declares no conflict of interest.*

## REFERENCES

1. Nguyen DC, Tam LN, Phan DH, Nguyen TC, Duy DN, Xuan QN. Using drone and ai application for power transmission line inspection and maintenance: A case study in vietnam. Intelligent Computing 2023;711;684–98. https://doi.org/10.1007/978-3-031-37717-4_44.
2. Singh G, Stefenon SF, Yow KC. Interpretable visual transmission lines inspections using pseudo-prototypical part network. Machine Vision and Applications 2023; 34(3): 41. https://doi.org/10.1007/s00138-023-01390-6.
3. Shafi I, Mazhar MF, Fatima A, Alvarez RM, Miró Y, Espinosa JCM, et al. deep learning-based real time defect detection for optimization of aircraft manufacturing and control performance. Drones 2023; 7(1):31. https://doi.org/10.3390/drones7010031.
4. Seo D, Kim J, Park S. An Experimental Study on defect detection of anchor bolts using non-destructive testing techniques. Materials 2023; 16(13): 4861. https://doi.org/10.3390/ma16134861.
5. Luo P, Wang B, Wang H, Ma F, Ma H, Wang L. An ultrasmall bolt defect detection method for transmission line inspection. IEEE Transactions on Instrumentation and Measurement 2023; 72: 1–12. https://doi.org/10.1109/TIM.2023.3241994.
6. Dong K, Shen Q, Wang C, Dong Y, Liu Q, Lu Z, et al. Improved swin transformer-based defect detection method for transmission line patrol inspection images. Evolutionary Intelligence 2023 https://doi.org/10.1007/s12065-023-00837-z.
7. Liu Y, Liu D, Huang X, Li C. Insulator defect detection with deep learning: A survey. IET Generation, Transmission & Distribution 2023; 17(16): 3541–58. https://doi.org/10.1049/gtd2.12916.
8. Wu Y, Cao H, Yang G, Lu T, Wan S. Digital twin of intelligent small surface defect detection with cyber-manufacturing systems. ACM Transactions on Internet Technology 2023; 23(4): 1–20. https://doi.org/10.1145/3571734.
9. Han G, Yuan Q, Zhao F, Wang R, Zhao L, Li S, et al. An improved algorithm for insulator and defect detection based on YOLOv4. Electronics 2023; 12(4): 933. https://doi.org/10.3390/electronics12040933.
10. Manaz H F, Banu R N, BK, A OP. transmission line quality inspection using ai. 2024 third international conference on intelligent techniques in control, Optimization and Signal Processing (INCOS) 2024; 1–5. https://doi.org/10.1109/INCOS59338.2024.10527492.
11. Ahmed MdF, Mohanta JC. Autonomous site inspection of power transmission line insulators with unmanned aerial vehicle system. Electric Power Components and Systems 2024: 1–24. https://doi.org/10.1080/15325008.2024.2313588.
12. Benelmostafa BE, Aitelhaj R, Elmoufid M, Medromi H. Detecting broken glass insulators for automated UAV power line inspection based on an improved YOLOv8 model. International Conference on Advanced Intelligent Systems for Sustainable Development 2023; 15(11): 309-321. https://doi.org/10.1080/15325008.2024.2313588.
13. Mokhtar MIM, Basri AA, Basri EI, Sultan MTH. Defect detection image processing for drone inspection on wide-body aircraft surface. E3S Web of Conferences 2024; 477: 00100. https://doi.org/10.1051/e3sconf/202447700100.

14. Saberironaghi A, Ren J, El-Gindy M. Defect detection methods for industrial products using deep learning techniques: A review. Algorithms 2023; 16(2): 95. https://doi.org/10.3390/a16020095.
15. Chatzargyros G, Papakonstantinou A, Kotoula V, Stimoniaris D, Tsiamitros D. UAV Inspections of power transmission networks with ai technology: a case study of lesvos Island in Greece. Energies 2024; 17(14): 3518. https://doi.org/10.3390/en17143518.
16. Souza BJ, Stefenon SF, Singh G, Freire RZ. Hybrid-YOLO for classification of insulators defects in transmission lines based on UAV. International Journal of Electrical Power & Energy Systems 2023; 148: 108982. https://doi.org/10.1016/j.ijepes.2023.108982.
17. Syu JH, Lin JCW, Srivastava G, Yu K. A comprehensive survey on artificial intelligence empowered edge computing on consumer electronics. IEEE Transactions on Consumer Electronics 2023;69(4):1023–34. https://doi.org/10.1109/TCE.2023.3318150.
18. Hussain M. YOLO-v1 to YOLO-v8, the Rise of YOLO and its complementary nature toward digital manufacturing and industrial defect detection. Machines 2023; 11(7): 677. https://doi.org/10.3390/machines11070677.
19. Bhuiyan MR, Uddin J. Deep transfer learning models for industrial fault diagnosis using vibration and acoustic sensors data: A review. Vibration 2023; 6(1): 218–38. https://doi.org/10.3390/vibration6010014.
20. Silitonga D, Rohmayanti SAA, Aripin Z, Kuswandi D, Sulistyo AB, Juhari. Edge Computing in E-commerce Business: Economic Impacts and Advantages of Scalable Information Systems. ICST Transactions on Scalable Information Systems 2023;11(1) https://doi.org/10.4108/eetsis.4375.
21. Bourechak A, Zedadra O, Kouahla MN, Guerrieri A, Seridi H, Fortino G. At the confluence of artificial intelligence and edge computing in iot-based applications: A review and new perspectives. Sensors 2023; 23(3): 1639. https://doi.org/10.3390/s23031639.
22. Pal S, Roy A, Shivakumara P, Pal U. Adapting a swin transformer for license plate number and text detection in drone images. Artificial Intelligence and Applications 2023; 1(3): 145–54. https://doi.org/10.47852/bonviewAIA3202549.
23. Raeisi-Varzaneh M, Dakkak O, Habbal A, Kim BS. Resource scheduling in edge computing: architecture, taxonomy, Open Issues and Future Research Directions. IEEE Access 2023; 11: 25329–50. https://doi.org/10.1109/ACCESS.2023.3256522.
24. Raith P, Nastic S, Dustdar S. Serverless edge computing—where we are and what lies ahead. IEEE Internet Computing 2023; 27(3): 50–64. https://doi.org/10.1109/MIC.2023.3260939.
25. Alnaim AK, Alwakeel AM. Machine-learning-based iot–edge computing healthcare solutions. Electronics 2023;12(4):1027. https://doi.org/10.3390/electronics12041027.

**Xi CHEN**
He received bachelor's degree from Northeast Electric Power University in 2009. At present, he works in Fangchenggang Power Supply Bureau of Guangxi Power Grid Co., Ltd., and is responsible for transmission operation and transmission maintenance management. His main research interests are drone technology, power transmission operation and maintenance.
e-mail: leng909210257@126.com

**Xumeng CHENG**
He received bachelor's degree from Guangxi University in 2014. At present, he works in Fangchenggang Power Supply Bureau of Guangxi Power Grid Co., Ltd., and is responsible for substation operation and standardized management. His main research interests are substation management and safety control of power production operations.
e-mail: zhangl0303@126.com

**Nengcheng WU**
He received bachelor's degree from Henan University of Urban Construction in 2009. At present, he works in Fangchenggang Power Supply Bureau of Guangxi Power Grid Co., Ltd. as a senior operator of the electrical test class of the substation management office. His main research interests are high voltage detection technology.
e-mail: manzaiyang@yeah.net

**Xuanyou LIU**
He obtained bachelor's degree from Guangxi Electric Power Vocational and Technical College in 2011. At present, he works in Fangchenggang Power Supply Bureau of Guangxi Power Grid Co., Ltd. as the leader of the intelligent operation team. His main research area is drone technology
e-mail: xushoudong1979@163.com